Carbohydrate Polymers 157 (2017) 303–310

Contents lists available at ScienceDirect

Carbohydrate Polymers

journal homepage: www.elsevier.com/locate/carbpol

Rheological properties of nanocrystalline cellulose suspensions

Yang Chen[a,b], Chunjiang Xu[a,b], Jing Huang[a,b], Defeng Wu[a,b,*], Qiaolian Lv[a,b]

[a] School of Chemistry & Chemical Engineering, Yangzhou University, Jiangsu 225002, PR China
[b] Provincial Key Laboratory of Environmental Engineering & Material, Jiangsu 225002, PR China

ARTICLE INFO

Article history:
Received 11 July 2016
Received in revised form 1 September 2016
Accepted 3 October 2016
Available online 4 October 2016

Keywords:
Nanocrystalline cellulose (NCC)
Suspension
Polymer solution
Rheology

ABSTRACT

Rheological behavior, including linear and nonlinear, as well as transient rheology of nanocrystalline cellulose (NCC) suspensions was studied in this work. Two kinds of polymer solutions, aqueous poly(vinyl alcohol) (PVA) with flexible chain structure and aqueous carboxymethyl cellulose (CMC) with semi-rigid chain structure, were used as the suspension media to further explore the role that the interactions among NCC and polymers played during shear flow. The results reveal that NCC has lower values of percolation threshold in the PVA solution than in the CMC one during small amplitude oscillatory shear (SAOS) flow because the flexible PVA chain has higher adsorbed level onto NCC particles than the negatively charged semi-rigid CMC chain, which is further confirmed by the Fourier transformed infrared (FT-IR) spectroscopy tests. As a result, the NCC suspension shows a weak strain overshoot in PVA solution during large amplitude oscillatory shear (LAOS) flow, which cannot be seen on the one in CMC solution. During startup shear flow, both of these two suspensions show evident stress overshoot behavior with the strain-scaling characteristics, indicating the formation of ordered long-term structure of rod-like NCC particles with self-similarity during flow. However, NCC suspension have far stronger stress overshoot response in CMC solution relative to the one in PVA solution. A possible synergy mechanism between NCC and CMC chain is hence proposed.

1. Introduction

As typical biomass with a wide variety of applications, cellulose has attracted much attention in recent years because of sharply increasing demand for renewability and sustainability. In particular, considerable effort has been devoted over the past decades to the study of nanocrystalline cellulose (NCC), because this kind of nanomaterial has high surface area, low density and good mechanical strength, with availability, biodegradable and non-toxic nature (Habibi, Lucia, & Rojas, 2010). Nowadays NCC has gained many successful applications in both the industrial and daily use fields, such as drug delivery excipients, reinforcements in polymer composites and adhesives, as well as personal care products, e.g. hair conditioners and shampoos (Brinchi, Cotana, Fortunati, & Kenny, 2013).

To those applications, especially to the drug carriers and the electronic fields, the rheology of NCC suspensions is very important. Therefore, the rheological properties, especially the linear flow behavior and steady shear response of the NCC suspension systems in water and in polymer solutions, have been explored up to now (Brinchi et al., 2013). In general, the negatively charged NCC particles can form stable aqueous dispersions because of the electrostatic repulsion among individual NCCs (Bercea & Navard 2000; Lasseuguette, Roux, & Nishiyama, 2008; Liu, Chen, Yue, Chen, & Wu, 2011). In this case, the rheological responses of aqueous NCC suspensions are mainly dominated by the short-range structural aspects of rod-shaped NCC particles such as aspect ratio and surface properties, and also by their long-range structure such as orientation state of particles and hydrodynamic particle–particle interactions, which is closely related to the concentration and surface charge of NCC particles (Puisto, Illa, Mohtaschemi, & Alava, 2012; Shafiei-Sabet, Hamad, & Hatzikiriakos, 2012; Noroozia, Grecova, & Shafiei-Sabet, 2014; Derakhshandeh, Petekidis, Shafiei-Sabet, Hamad, & Hatzikiriakos, 2013; Jin et al., 2015; Lenfant, Heuzey, van de Ven, & Carreau, 2015; Lu, Hemraz, Khalili, & Boluk, 2014).

In polymer solutions, the situation becomes much more complicated. The dispersion stability of NCC particles is affected by both adsorbed and non-adsorbed polymers (Boluk, Zhao, & Incani, 2012). In this kind of suspensions, polymer chain can cause two types of steric interactions among NCC particles: either bridging by adsorption of polymer chain on NCC particle surface

* Corresponding author at: School of Chemistry & Chemical Engineering, Yangzhou University, Jiangsu 225002, PR China.
E-mail address: dfwu@yzu.edu.cn (D. Wu).

http://dx.doi.org/10.1016/j.carbpol.2016.10.002
0144-8617/

or depletion by non-adsorbing polymers, both resulting in the enhanced stress response and system elasticity (El Kissi et al., 2008; Gomez Martinez, Stading, & Hermansson, 2013; Mihranyan, 2013). Besides, it is expectable that the surface charge of polymers should also have large influence on the colloidal stability and rheological response of NCC suspensions, which is supposed to be very similar with the case of the suspensions containing spherulitic or platelet-like particles (Sjoberg, Bergstrom, Larsson, & Sjostrom, 1999). However, for the NCC suspension in polymer solutions, no literature report can be found on this issue.

Moreover, the reported rheological studies on the NCC suspension systems in water or in polymer solutions mainly focus on the linear flow behavior, or the steady shear responses. The former is limited in a quite narrow stress or strain region, which is far less than the engineering levels; and the latter can merely give the final stress or strain levels, and cannot reveal the transient response that is closely related to the structure evolution during shear flow. Therefore, in this work, both the nonlinear and transient rheology of NCC suspensions were studied deeply, together with the linear dynamic rheology. Two kinds of polymer solutions, electrically neutral aqueous poly(vinyl alcohol) with flexible chain structure and negatively charged aqueous carboxymethyl cellulose with semi-rigid chain structure, were used as the suspension media to further explore the role that the NCC-polymer interactions played during flow. The main objective of this work is to make a full and deep study on the flow behavior of NCC suspension in polymer solutions, and to provide useful information on the applications of NCC suspension systems.

2. Experiment

2.1. Materials

Poly(vinyl alcohol) (PVA1788) used in this work is a commercial product of Aladdin Industrial Co. Ltd. (P.R. China) with the molecular weight of 44.05×10^3 g mol^{-1} (polydispersity index (PDI = 2.25)) and the density of 1.3×10^3 kg m^{-3}. Its degree of alcoholysis (DA) is about 87.0–89.0% (mol mol^{-1}). Carboxymethyl cellulose (CMC) with the molecular weight of 260.24×10^3 g mol^{-1} (PDI = 1.37) and the density of 1.6×10^3 kg m^{-3} was also purchased from Aladdin Industrial Co. Ltd., which has a viscosity of 600–1000 mPa s for the solution with concentration of 2 wt% at 25 °C. Its charge density is about -15.82 mc m^{-2}. The microcrystalline cellulose (MCC) used for the preparation of NCC was purchased from Sinopharm Chemical Reagent Co. Ltd. (P. R. China), with the degree of polymerization (DP) of 210–240. The average length and diameter of MCC are 20–100 μm and 10–20 μm, respectively.

2.2. Preparation of NCC and its suspensions

NCC aqueous suspensions (deionized water was used) were prepared according to the procedure reported in the previous work (Bai, James, & Li, 2009; Chen et al., 2015). TEM image of as-obtained NCC particles is shown in Fig. 1. Their average diameter and length are about 20 nm and 300 nm, respectively. The PVA or CMC was then dissolved in the aqueous NCC suspensions, with stirring at moderate level at 30 °C for 12 h, followed by the 12 h rest for defoaming. Because CMC is hard to be fully dissolved in water at the higher concentration level (>1 wt%), its concentration is fixed as 1 wt% in the suspension system. The PVA concentration is determined as 10 wt% because at this concentration the PVA solution has the same viscosity level as the CMC solution (Fig. S1 of the Supplementary information), which favors rheological property comparison of two kinds of NCC suspensions. The NCC loadings vary from 0.1 to 3.0 wt%. The film samples casted from suspensions are characterized using atomic force microscope and the results are shown in Fig. S2 of the Supplementary information (the bumps or dark parts on the force images are part of the NCC particles embedded by polymer matrix because NCC has higher modulus than polymer matrix (Xu et al., 2016)).

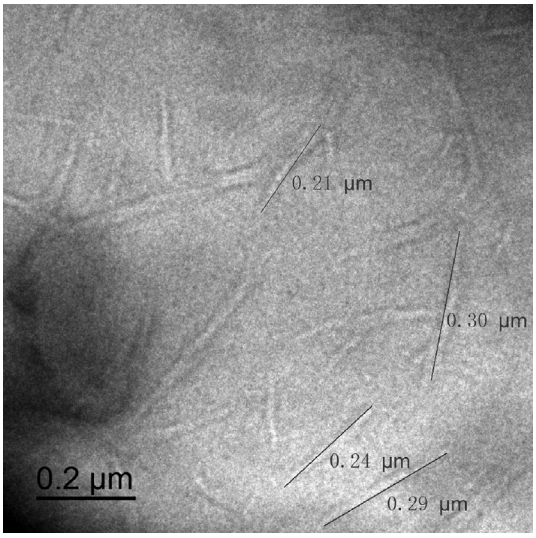

Fig. 1. TEM image of NCC particles with the scale bar of 0.2 μm.

2.3. Morphological characterizations

The dispersion of NCC in the cast film of PVA and CMC was detected using atomic force microscope (AFM). An Icon AFM (Bruker Co. Ltd, Santa Barbara, USA) was operated in the quantitative nanomechanical mapping mode (QNM). Silicon AFM probes were used (tip radius < 8 nm, force constant 40 N m^{-1}, resonance frequency 300 kHz) to acquire images in air at room temperature. Line scan rates were set as lower at 256 lines per frame with a scanning rate of 1 Hz. Image processing was performed with the NanoScope Analysis software.

2.4. Structure characterizations

Fourier transformed infrared spectroscopy (FT-IR) was used to identify the possible interactions between NCC particles and polymers. Infrared absorption spectra were recorded in the wavelength region of 4000–600 cm^{-1} using a Bruker IFS66/S FT-IR spectrophotometer (Germany). All the FT-IR spectra were obtained by repeating 64 scans at room temperature with the resolution of 2 cm^{-1}. The hydrodynamic radius of NCC in water and in the polymer solutions was determined by a ZEN360 dynamic light scattering apparatus (DLS, Malvern Co. Ltd., United Kingdom) at 25 °C. The scattering angle and operating wavelength were 90° and 632 nm, respectively. The zeta potential (ζ) (also measured by DLS apparatus) was calculated from the velocity of the particles under a given electrical current. Its values were obtained along with the DLS tests.

2.5. Rheological measurements

The rheological tests were performed on a rotational rheometer (HAAKE RS600, Thermo Electron Co., USA) equipped with a parallel plate geometry (60 mm diameter plates). The samples were hold at 10–20 °C for 3 min in the parallel plate fixture to eliminate residual thermal and stress histories, and then experienced various kinds of shear flows (the water is volatile and therefore, a lower temperature range, 10–20 °C, was chosen for rheological tests). During

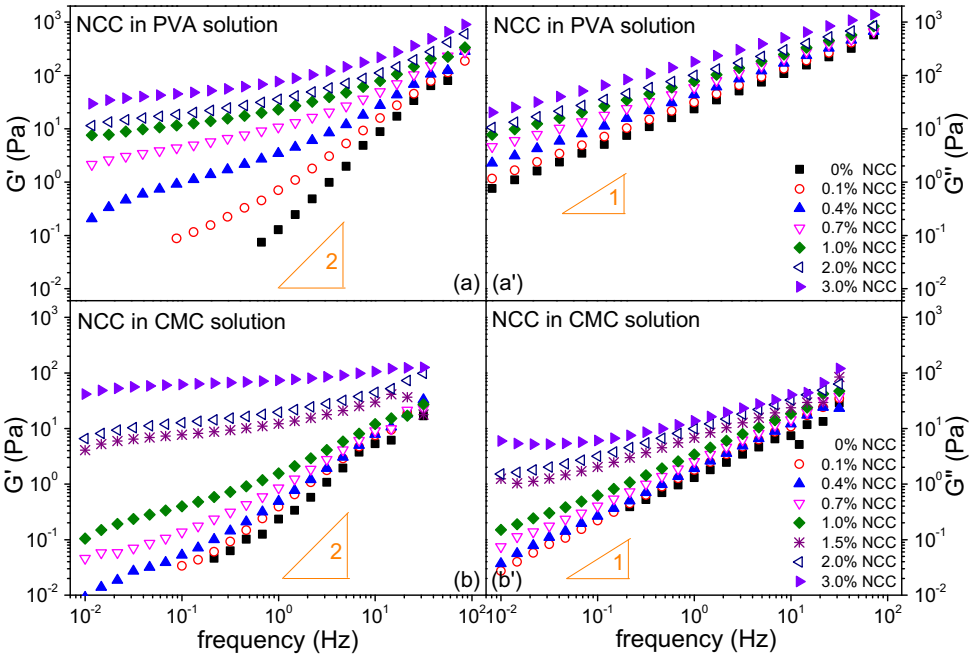

Fig. 2. Dynamic storage modulus (G') (left) and loss modulus (G'') responses (right) for the suspension systems of (a, a′) NCC in PVA solution and (b, b′) in CMC solution measured at 10 °C.

steady and transient shear flow, the stress or viscosity responses to the shear rates were recorded. In the transient rheological measurements, the startup of shear was applied. Firstly, the sample experienced shear flow at the predetermined rates, during which the transient shear stress was monitored until the stress response tended to be steady. The shear rate levels were determined according to the results of steady shear measurements. In the dynamic rheological measurements, the dynamic stress sweep was carried out firstly to determine a common linear region. Then, the dynamic frequency sweep was performed under the small amplitude oscillatory shear (SAOS) flow.

3. Results and discussion

3.1. Linear rheology of NCC suspension in aqueous polymer solutions

Fig. 2 gives linear dynamic modulus responses of two kinds of NCC suspensions. Both show monotonous increase of modulus values with increase of NCC loadings, which is believed to be attributed to the increased particle–particle interactions (Boluk et al., 2012; Shafiei-Sabet et al., 2012). It is well known that the transition from dilute to semi dilute concentration for a suspension or a particles filled system occurs at the volume fraction of $\phi \leq (\pi/4)(d/L)^2$ where d is the diameter and L the length of particles (Chatterjee & Krishnamoorti (2007), Chatterjee, Yurekli, Hadjiev, & Krishnamoorti (2005) and Wu, Wu, Zhang (2007)). For the current NCC suspensions, the transition critical value from dilute to semi dilute is ca. 0.6 wt%. That means that the systems with lower NCC loadings (0.1–0.4 wt%) are dilute, while others semi dilute or even more. Therefore, the dynamic response of systems is still dominated by the viscous flow at the lower NCC loading levels because low-frequency G'' is higher than G', suggesting a rather weak hydrodynamic interactions among the NCC particles. At the higher loading levels, the shear flow is dominated by elastic deformation because G' shows higher values than G'' at the low frequency region. This is attributed to the percolation of NCC particles in the polymer solutions, which is also called gelation or gel-like flow behavior (Shafiei-Sabet et al., 2012).

The percolation threshold of these two suspension systems can be determined by van Gurp-Palmen (v-GP) plots (Van Gurp & Palmen, 1998), as shown in Fig. 3. 45° phase angle (δ) is used as the criteria to evaluate the liquid-to-solid-like transition of a suspension system during SAOS flow. It is clear that the suspension system has the phase angle lower than 45° as the NCC loading level achieves up to 0.7 wt% (Fig. 3a), indicating that NCC particles are percolated in PVA solution with a threshold value of about 0.7 wt%. It is well known that the hydrodynamic volume fraction of particles in a suspension system is closely related with their aspect ratio during shear flow (Djalili-Moghaddam & Toll, 2006). The higher the aspect ratio of particles, the lower their percolation threshold in a suspension system. The effective volume fraction (ϕ_{eff}) of NCC particles can be calculated by the Quemada (Quemada, 1998) modified Krieger (Krieger, 1972) equation:

$$\eta_r = \left(1 - \frac{\phi_{\text{eff}}}{\phi_m}\right)^{-q} \quad (1)$$

where η_r is the relative viscosity, ϕ_m the maximum volume fraction, and q decided by the intrinsic viscosity $[\eta]$ ($q = [\eta]\phi_m$). In the PVA solution, ϕ_{eff} values of NCC are about 17.3 vol% at the loading levels of 0.7 wt%. It should be indicated that ϕ_{eff} here is a hydrodynamic variable, which is closely related to the aspect ratio of NCC and shear flow, but not the real volume fraction. Detailed calculation method can be found elsewhere (Wu et al., 2010). This threshold (0.7 wt%) is far lower than that observed on the aqueous NCC suspensions (~7 wt%) (Shafiei-Sabet et al., 2012) but almost the same level as that reported on the colloidal NCC suspension in the polymer solutions (~0.6 wt%) (Boluk et al., 2012). It should be attributed to the polymer-NCC percolation instead of simple NCC-NCC one because of strong interactions between polymer chain and NCC particles, which will be discussed later (in the following FT-IR discussion section).

In the CMC solution, the threshold value of NCC ranges in 1.0-1.5 wt%, close to 1.0 wt% (Fig. 2b), which is larger than that in the PVA one. This is interesting because relative to the PVA chain, CMC

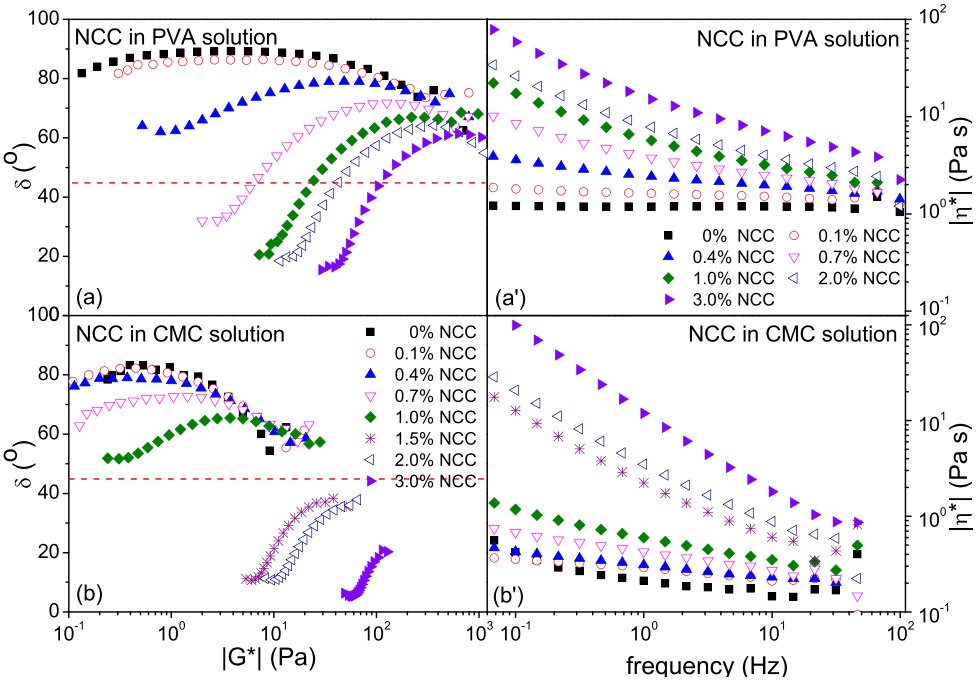

Fig. 3. (a, b) v-GP plots of loss angle (δ) versus dynamic complex modulus ($|G^*|$) (left) and (a′, b′) complex viscosity responses (right) for the suspensions of NCC in PVA solution and in CMC solution measured at 10 °C.

Table 1
The values of zeta potential (ζ) (10 °C) of the neat PVA and CMC aqueous solutions and NCC suspensions with various NCC loadings.

ζ (mV)	NCC	PVA solution[a]	CMC solution[a]	NCC in PVA solution	NCC in CMC solution
	−30.9	−0.2	−92.0	−1.21[b]/−1.58[c]	−60.5[b]/−63.9[c]

[a] PVA and CMC concentrations in aqueous solutions are 10 wt% and 1 wt%, respectively.
[b] NCC loading in the suspensions is 0.1 wt%.
[c] NCC loading in the suspensions is 1.0 wt%.

chain is supposed to have stronger affinity to NCC particles due to their similar chain structure. This threshold difference is caused by the difference in the surface properties and chain flexibility between PVA and CMC. The zeta potential (ζ) values of the neat polymer aqueous solutions and NCC suspensions are summarized in Table 1. Clearly, neat CMC aqueous solution is negatively charged, while PVA one almost electrically neutral. This means that semi-rigid CMC chain has much stronger electrostatic repulsion to the negatively charged NCC particles relative to the flexible PVA chain. In other words, PVA is an adsorbable polymer to NCC in the aqueous suspension, while CMC not. This is further confirmed by the FT-IR tests.

Fig. 4 gives FT-IR spectra for the PVA/NCC and CMC/NCC systems. The bands around 1800–1500 cm^{-1} correspond to C—O and C═O vibration for PVA (Shalumon et al., 2009) and CMC chains (Li, Sun, & Wu, 2009), respectively. Both show evident downshift in the presence of NCC particles, which is believed to be attributed to the formation of strong interactions between polymer chain and NCC particle surface via hydrogen bonding (Fan et al., 2015; Li et al., 2009; Shalumon et al., 2009; Zhang, Dehghani-Sanij, & Blackburn, 2008) or dipole–dipole coupling interactions (Zhang et al., 2008; Wu, Wu, Wu, Xu, & Zhang, 2007). At the same NCC loading levels, however, C═O stretching peak of CMC shifts from 1631 to 1625 cm^{-1} merely by about 6 cm^{-1}, while C—O vibration peak of PVA from 1640 to 1607 cm^{-1} by about 33 cm^{-1}. It should be mentioned that concentration level of 1.0 wt% CMC is already saturated for the adsorption of polymer chain onto NCC particles because zeta potential values are nearly independent on the NCC loadings at current concentration of CMC (1 wt%) (Table 1). Therefore, more remarkable peak downshift indicates that the PVA chain has far stronger interactions with NCC in a suspension system relative to the CMC chain.

This is reasonable because on the one hand, there is no strong electrostatic repulsion between PVA chain and NCC particles; and on the other hand, flexible PVA chain is much easier to be adsorbed onto NCC due to strong hydrogen bonding, as compared with rigid CMC chain. This is further confirmed by the increased hydrodynamic size of NCC (measured by DLS) in the PVA solution relative to the case in the CMC one, as can be seen in Fig. S3 of the Supplementary information (the average diameters here can only be used for value comparison, and is physically meaningless somehow because the tested suspensions are not dilute enough, despite of viscosity calibration). Therefore, the dispersion state of NCC in these two solutions can be proposed by the schematic diagrams shown in Fig. 5. The adsorbed PVA chains have bridging effect, promoting the formation of flocculation structure of NCC (see the parts indicated by the arrows), which favors the formation of percolation network of NCC in the PVA solution at the relatively lower loadings. The presence of non-adsorbed CMC chains, however, have strong electrostatic repulsion with NCC, merely with lower adsorption level, The resulted shielding effect, therefore, makes NCC particles percolated at the higher loading levels.

3.2. Nonlinear rheology of NCC suspension in aqueous polymer solutions

Unlike SAOS flow, large amplitude oscillatory shear (LAOS) one is not restricted in a narrow linear strain range, and therefore, can

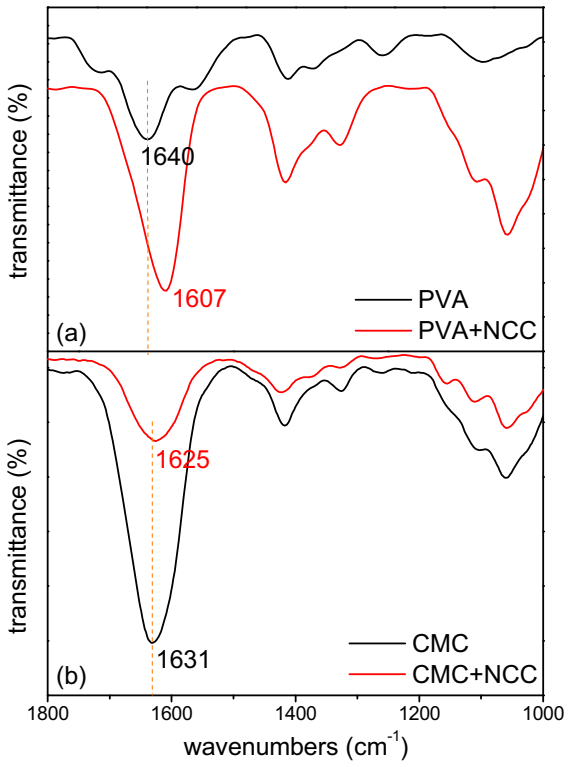

Fig. 4. FT-IR spectra of (a) neat PVA and its NCC system and (b) neat CMC and its NCC system.

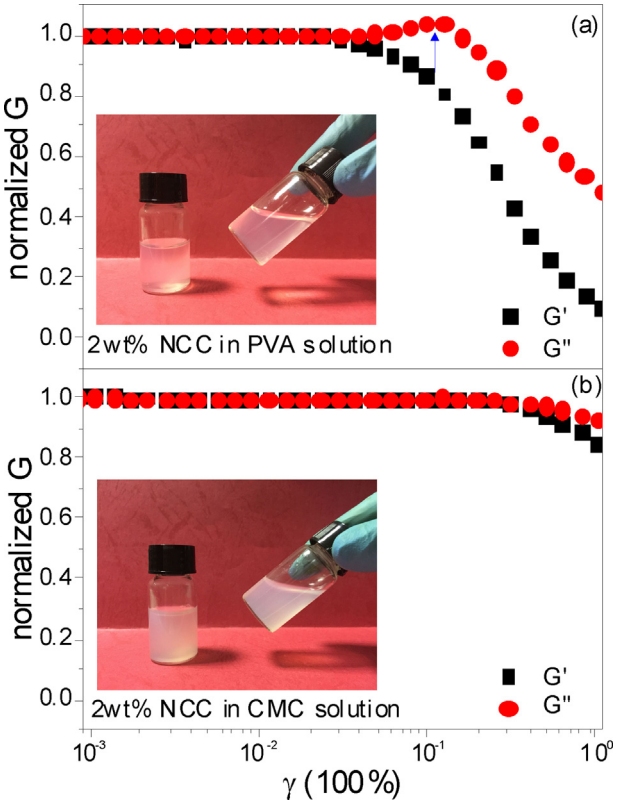

Fig. 6. Normalized dynamic storage modulus (G') and loss modulus (G'') responses for (a) NCC (2 wt%) in PVA solution and (b) in CMC solution measured at 10 °C. The inset graphs reveal the flowability of the two tested suspensions and the arrow indicates the overshoot.

provide some useful information on the dispersion or polymer-particle interactions of a suspension system (Sim, Ahn, & Lee, 2003). Fig. 6 gives the normalized modulus responses (divided by the initial values at 10^{-3} Hz) for the two NCC suspension systems (2 wt%) (The flowability of two systems are shown in the inset graphs). In general, four types of strain behavior are commonly observed on polymeric materials during LAOS flow, namely strain thinning and hardening, weak and strong strain overshoot (Wu et al., 2011; Wan et al., 2005; Wu, Zhou, Yu, & Xie, 2005; Hyun, Kim, Ahn, & Lee, 2002). Strain thinning is most easily observed on the polymer solutions and melts as well as most of polymer composites. This type is believed to have similar origin to shear thinning, which is due to the reduced local drag caused by chain orientation or alignment of microstructures. The CMC solution reveals such typical strain thinning behavior in the presence of NCC particles, as can be seen in Fig. 6b. However, a weak strain overshoot is observed on the nonlinear flow of PVA solution in the presence of NCC (Fig. 6a).

The 'weak' means that only G'' shows overshoot while G' does not (Hyun et al., 2002). It is easily observed on the polymers with long side chains (Wu et al., 2011) or multiphase systems (Wan et al., 2005; Wu, Zhou, Yu et al., 2005) with strong interactions among different phases. The strain overshoot is caused by the formation of weak structural complexes in the highly extended structure by hydrogen bonding, strong physical interactions, etc. As an external strain with large amplitude is imposed, the complex structure

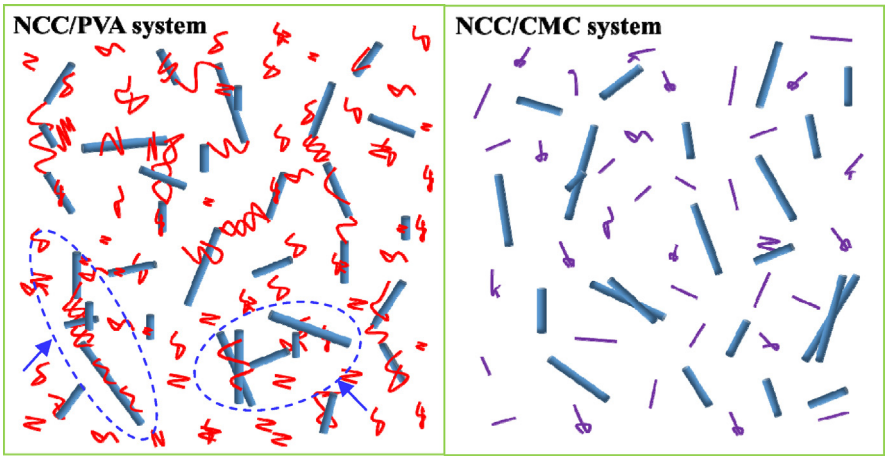

Fig. 5. Schematic diagrams of dispersion state of NCC particles in PVA (left) and CMC (right) aqueous solutions (blue rods are NCC particles, red curves PVA chains, and purple short line CMC chains). (For interpretation of the references to color in this figure legend, the reader is referred to the web version of this article.)

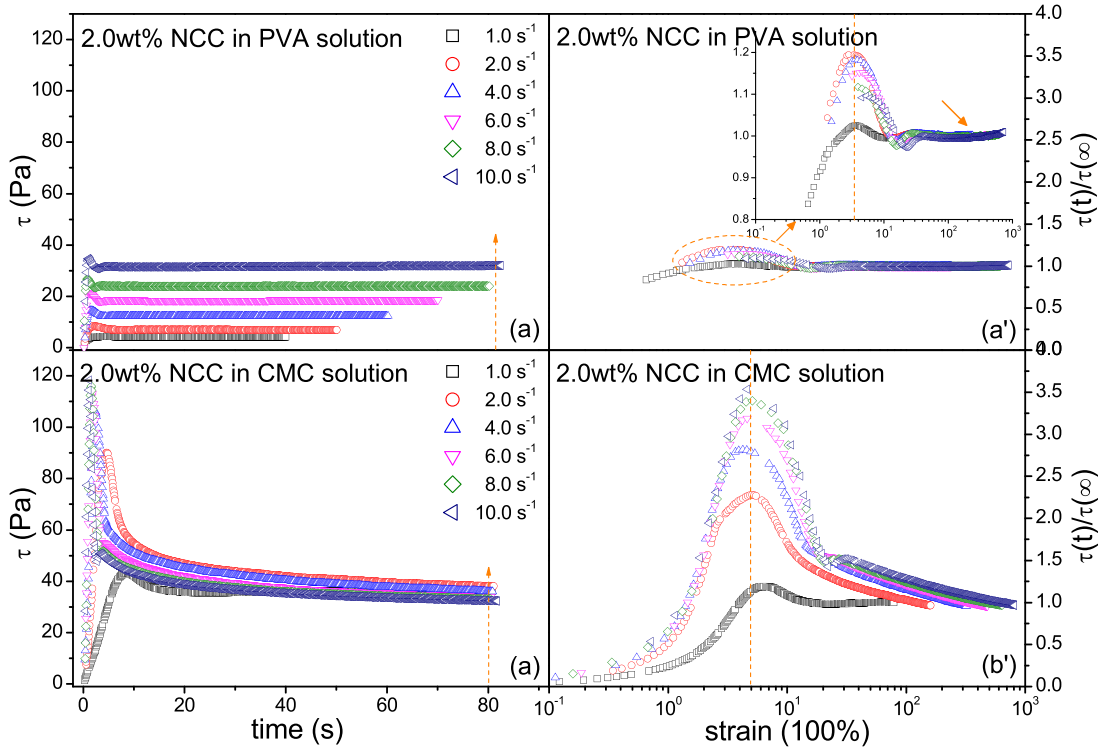

Fig. 7. Transient shear stress responses as the function of time (left) and normalized values as the function of strain (right) for the suspension systems of NCC (2 wt%) in (a, a′) PVA solution and (b, b′) CMC solution to the startup of shear flows at various rates (10 °C) (the arrow indicates nonzero residual stress responses).

resists against deformation up to a certain level of strain, leading to the increase of G''. Then, those weak associations are destroyed by large deformation over the critical strain, and G'' decreases sharply as a result. As schematically shown in Fig. 5, NCC particles can form flocculated structure by the way of adsorption of PVA chains and as-resulted bridging effect. These structural complexes are believed to the origination of weak strain overshoot during LAOS flow (Wu, Zhou, Yu et al., 2005). Clearly, LAOS flow confirms that NCC particles have stronger interactions with flexible PVA chain than with semi-rigid CMC chain in suspension systems.

3.3. *Transient rheology of NCC suspension in aqueous polymer solutions*

Transient stress response is closely related to the structural evolution in a multiphase system (Hyun et al., 2002). Fig. 7 gives transient stress responses to the startup of shear flow for the two suspension systems with 2.0 wt% NCC (responses of the suspensions with other loading levels can be seen in Fig. S4 of the Supplementary information). Both show evident overshoot behavior during stress development, and the overshoot levels increase with increasing flow rates. Martoia et al. (2015) reported similar stress evolution during start-up flow of aqueous cellulose nanofibril (CNF) suspensions. They proposed that this flow behavior was probably related to the heterogeneous elastoviscoplastic deformation of the initially entangled nanostructure of the CNF suspensions. For the NCC aqueous suspensions in this work, the stress overshoot and its damping with time are attributed to the energy storage of flocculated and percolated structures of NCC and the subsequent energy dissipation caused by the relaxation of those structures along flow direction (Wu et al., 2010).

It is seen that the normalized stress responses at various shear rates scale with strain (Fig. 7a′, b′) for both of these two suspension systems, and the maximum of all overshoots approximately appears at the strain of 4–5. Similar strain-scaling behavior has also been observed on many kinds of multiphase systems such as polymer-carbon nanotube suspensions (Wu, Wu, Wu et al., 2007), nanoclay filled polymer nanocomposites (Wu, Zhou, Zheng, Mao, & Zhang, 2005; Solomon, Almusallam, Seefeldt, & Varadan, 2001; Okamoto, Morita, Kim, Kotaka, & Tateyama, 2001; Wu, Wu, Wu, & Zhang, 2006), and partly-crosslinked (Wu et al., 2011) or long chain branched polymers (Wu, Wu, Wu et al., 2007), which is believed to be attributed to formation of the structure with the characteristics of self-similarity, such as the percolation network (Okamoto et al., 2001; Wu et al., 2006) or the liquid crystalline-like structure (Solomon et al., 2001; Sui & McKenna, 2007). It has been reported that like other rod-like particles, NCC can also form nematic liquid crystalline domains (Noroozia et al., 2014; Derakhshandeh et al., 2013) or liquid crystalline-like structure along with shear flow (Lu et al., 2014) in their suspensions. On the other hand, the percolated NCC network is also of self-similarity, like other the percolated rod-like or platelet-like nanoparticle networks (Okamoto et al., 2001; Solomon et al., 2001; Sui & McKenna, 2007; Wang et al., 2015; Wu et al., 2006; Wu, Wu, Wu et al., 2007; Wu, Zhou, Yu et al., 2005). These two aspects together result in an evident strain-scaling overshoot behavior of NCC aqueous suspensions as the stress approaches to the steady state during shear flow.

It is interesting that at the same rate level, NCC/CMC suspension shows far stronger overshoot response than NCC/PVA one, which is contrary to the percolation threshold trend discussed in the linear rheology section. It is reported that the CMC aqueous solution itself can form the liquid crystalline structure during shear flow (Marsano, De Paz, Tambuscio, & Bianchi, 1998; Veen, Kuijk, Versluis, Husken, & Velikov, 2014), however, in this work, it cannot form the liquid crystalline phase at the current low concentration of CMC (1 wt%) (See the polarized optical image shown in Fig. S5 of the Supplementary information. Nothing is observed after shear flow.). A possible synergy mechanism between NCC and CMC is hence proposed here. As discussed in linear rheology section, CMC chain has much stronger electrostatic repulsion to the negatively

charged NCC particles than the PVA chain. In this case, the interactions among NCC particles themselves become weak because of shielding or dilution effect. On the other hand, semi-rigid chain structure of CMC means that it is not that possible to be adsorbed onto the surface of NCC. Therefore, the flocculation level of NCC in the CMC solution is far lower than that in the PVA one, as schematically shown in Fig. 5. Accordingly, NCC particles are easier to form ordered phase in the CMC solution. In other words, the synergistic effect between NCC particles and CMC chain results in stronger overshoot response of NCC/CMC suspension system than that of NCC/PVA one.

Besides, a nonzero residual stress behavior is seen on the NCC/PVA system (arrow in Figs. 7 a′ and S4 of the Supplementary information) in long-time scale. It is attributed to rotation or roll-over relaxation of rod-like NCC particles at high shear rates because of drawing and dragging effects caused by strong interactions between PVA chain and NCC particles (Wang et al., 2015; Wu et al., 2006). This behavior is not seen on the NCC/CMC system, confirming the lower adsorption level between CMC chain and NCC, and as-resulted lower flocculation level of NCC. Clearly, it is in accordance with the level difference of stress overshoot between these two systems. Therefore, transient rheology can reveal more information on the long-range structure of NCC and its relations with polymer-NCC interactions in a suspension system under shear flow.

4. Conclusions

NCC particles can be dispersed well in both the PVA and CMC aqueous solutions, forming stable suspensions. Relative to the semi-rigid CMC with negative charge, the flexible PVA has much stronger interactions with negatively charged NCC particles, leading to a lower percolation threshold of NCC in the PVA aqueous solution during SAOS flow and to a weak strain overshoot behavior during LAOS flow. Both are caused by the formation of flocculation structure of NCC. Besides, the two suspension systems show evident stress overshoot response during startup shear flow, revealing strain-scaling characteristics, which is caused by the formation of long-term ordered structure of NCC particles in the polymer solutions. But the overshoot level is very sensitive to the chain structure of used polymers and their interactions with NCC particles.

Acknowledgements

This work was supported by the research grants from the National Natural Science Foundation of China (51573156), the Prospective Joint Research Program of Jiangsu Province (BY2014117-01), as well as the Blue Project of Jiangsu Province.

Appendix A. Supplementary data

Supplementary data associated with this article can be found, in the online version, at http://dx.doi.org/10.1016/j.carbpol.2016.10.002.

References

Bai, W., James, H., & Li, K. C. (2009). A technique for production of nanocrystalline cellulose with a narrow size distribution. *Cellulose*, *16*, 455–465.
Bercea, M., & Navard, P. (2000). Shear dynamics of aqueous suspensions of cellulose whiskers. *Macromolecules*, *33*, 6011–6016.
Boluk, Y., Zhao, L. Y., & Incani, V. (2012). Dispersions of nanocrystalline cellulose in aqueous polymer solutions: Structure formation of colloidal rods. *Langmuir*, *28*, 6114–6123.
Brinchi, L., Cotana, F., Fortunati, E., & Kenny, J. M. (2013). Production of nanocrystalline cellulose from lignocellulosic biomass: Technology and applications. *Carbohydrate Polymers*, *94*, 154–169.
Chatterjee, T., & Krishnamoorti, R. (2007). Dynamic consequences of the fractal network of nanotube-poly(ethylene oxide) nanocomposites. *Physical Review E*, *75*, 050403.
Chatterjee, T., Yurekli, K., Hadjiev, V. G., & Krishnamoorti, R. (2005). Single-walled carbon nanotube dispersions in poly(ethylene oxide). *Advanced Functional Materials*, *15*, 1832–1838.
Chen, J. X., Xu, C. J., Wu, D. F., Sha, Y. L., Pan, K. R., Wang, L., et al. (2015). Insights into the nucleation role of cellulose crystals during crystallization of poly(β-hydroxybutyrate). *Carbohydrate Polymers*, *134*, 508–515.
Derakhshandeh, B., Petekidis, G., Shafiei-Sabet, S., Hamad, W. Y., & Hatzikiriakos, S. G. (2013). Ageing, yielding: And rheology of nanocrystalline cellulose suspensions. *Journal of Rheology*, *57*, 131–148.
Djalili-Moghaddam, M., & Toll, S. (2006). Fibre suspension rheology: Effect of concentration: Aspect ratio and fibre size. *Rheological Acta*, *45*, 315–320.
El Kissi, N., Alloin, F., Dufresne, A., Sanchez, J. Y., Bossard, F., D'Aprea, A., et al. (2008). Influence of cellulose nanofillers on the rheological properties of polymer electrolytes. *AIP Conference Proceedings*, *1027*, 87–89.
Fan, L. H., Yang, J., Wu, H., Hu, Z. H., Yi, J. Y., Tong, J., et al. (2015). Preparation and characterization of quaternary ammonium chitosan hydrogel with significant antibacterial activity. *International Journal of Biological Macromolecules*, *79*, 830–836.
Gomez Martinez, D., Stading, M., & Hermansson, A. M. (2013). Viscoelasticity and microstructure of a hierarchical softcomposite based on nano-cellulose and *k*-carrageenan. *Rheologica Acta*, *52*, 823–831.
Habibi, Y., Lucia, L. A., & Rojas, O. J. (2010). Cellulose nanocrystals: Chemistry, self-assembly and applications. *Chemical Reviews*, *110*, 3479–3500.
Hyun, K., Kim, S. H., Ahn, K. H., & Lee, S. J. (2002). Large amplitude oscillatory shear as a way to classify the complex fluids. *Journal of Non-Newtonian Fluid Mechanics*, *107*, 51–65.
Jin, Y., Hengl, N., Baup, S., Pignon, F., Gondrexon, N., Sztucki, M., et al. (2015). Ultrasonic assisted cross-flow ultrafiltration of starch and cellulose nanocrystals suspensions: Characterization at multi-scales. *Carbohydrate Polymers*, *124*, 66–76.
Krieger, I. M. (1972). Rheology of monodisperse lattices. *Advances in Colloid and Interface Science*, *3*, 111–136.
Lasseuguette, E., Roux, D., & Nishiyama, Y. (2008). Rheological properties of microfibrillar suspension of TEMPO-oxidized pulp. *Cellulose*, *15*, 425–433.
Lenfant, G., Heuzey, M. C., van de Ven, T. G. M., & Carreau, P. J. (2015). Intrinsic viscosity of suspensions of electrosterically stabilized nanocrystals of cellulose. *Cellulose*, *22*, 1109–1122.
Li, W., Sun, B. J., & Wu, P. Y. (2009). Study on hydrogen bonds of carboxymethyl cellulose sodium film with two-dimensional correlation infrared spectroscopy. *Carbohydrate Polymers*, *78*, 454–461.
Liu, D. G., Chen, X. Y., Yue, Y. Y., Chen, M. D., & Wu, Q. L. (2011). Structure and rheology of nanocrystalline cellulose. *Carbohydrate Polymers*, *84*, 316–322.
Lu, A., Hemraz, U., Khalili, Z., & Boluk, Y. (2014). Unique viscoelastic behaviors of colloidal nanocrystalline cellulose aqueous suspensions. *Cellulose*, *21*, 1239–1250.
Marsano, E., De Paz, L., Tambuscio, E., & Bianchi, E. (1998). Cellulose methacrylate: Synthesis and liquid crystalline behaviour of solutions and gels. *Polymer*, *39*, 4289–4294.
Martoia, F., Perge, C., Dumont, P. J. J., Orgeas, L., Fardin, M. A., Manneville, S., et al. (2015). Heterogeneous flow kinematics of cellulose nanofibril suspensions under shear. *Soft Matter*, *11*, 4742–4755.
Mihranyan, A. (2013). Viscoelastic properties of cross-linked polyvinyl alcoholand surface-oxidized cellulose whisker hydrogels. *Cellulose*, *20*, 1369–1376.
Noroozia, N., Grecova, D., & Shafiei-Sabet, S. (2014). Estimation of viscosity coefficients and rheological functions of nanocrystalline cellulose aqueous suspensions. *Liquid Crystals*, *1*, 56–66.
Okamoto, M., Morita, S., Kim, Y. H., Kotaka, T., & Tateyama, H. (2001). Dispersed structure change of smectic clay/poly(methyl methacrylate) nanocomposites by copolymerization with polar comonomers. *Polymer*, *42*, 1201–1206.
Puisto, A., Illa, X., Mohtaschemi, M., & Alava, M. (2012). Modeling the rheology of nanocellulose suspensions. *Nordic Pulp & Paper Research Journal*, *27*, 277–281.
Quemada, D. (1998). Rheological model of complex fluids. I. The concept of effective volume fraction. *European Physical Journal*, 119–127 [AP-1]
Shafiei-Sabet, S., Hamad, W. Y., & Hatzikiriakos, S. G. (2012). Rheology of nanocrystalline cellulose aqueous suspensions. *Langmuir*, *28*, 17124–17133.
Shalumon, K. T., Binulal, N. S., Selvamurugan, N., Nair, S. V., Menon, D., Furuike, T., et al. (2009). Electrospinning of carboxymethyl chitin/poly(vinyl alcohol) nanofibrous scaffolds for tissue engineering applications. *Carbohydrate Polymers*, *77*, 863–869.
Sim, H. G., Ahn, K. H., & Lee, S. J. (2003). Large amplitude oscillatory shear behavior of complex fluids investigated by a network model: A guideline for classification. *Journal of Non-Newtonian Fluid Mechanics*, *112*, 237–250.
Sjoberg, M., Bergstrom, L., Larsson, A., & Sjostrom, E. (1999). The effect of polymer and surfactant adsorption on the colloidal stability and rheology of kaolin dispersions. *Colloids and Surface A*, *159*, 197–208.
Solomon, M. J., Almusallam, A. S., Seefeldt, K. F., & Varadan, P. (2001). Rheology of polypropylene/clay hybrid materials. *Macromolecules*, *34*, 1864–1872.
Sui, C. P., & McKenna, G. B. (2007). Nonlinear viscoelastic properties of branched polyethylene in reversing flows. *Journal of Rheology*, *51*, 341–365.
Van Gurp, M., & Palmen, J. (1998). Time-temperature superposition for polymeric blends. *Journal of Rheology Bulletin*, *67*, 5–8.

Veen, S. J., Kuijk, A., Versluis, P., Husken, H., & Velikov, K. P. (2014). Phase transitions in cellulose microfibril dispersions by high-energy mechanical deagglomeration. *Langmuir*, *30*, 13362–13368.
Wan, T., Clifford, M. J., Gao, F., Bailey, A. S., Gregory, D. H., & Somsunan, R. (2005). Strain amplitude response and the microstructure of PA/clay nanocomposites. *Polymer*, *46*, 6429–6436.
Wang, Y., Cheng, Y. X., Chen, J. X., Wu, D. F., Qiu, Y. X., Yao, X., et al. (2015). Percolation networks and transient rheology of polylactide composites containing graphite nanosheets with various thicknesses. *Polymer*, *67*, 216–226.
Wu, D. F., Wu, L., Wu, L. F., & Zhang, M. (2006). Rheology and thermal stability of polylactide/clay nanocomposites. *Polymer Degradation and Stability*, *91*, 3149–3155.
Wu, D. F., Wu, L., Zhou, W. D., Sun, Y. R., & Zhang, M. (2010). Relations between the aspect ratio of carbon nanotubes and the formation of percolation networks of biodegradable polylactide/carbon nanotube composites. *Journal of Polymer Science Part B: Polymer Physics*, *48*, 479–489.
Wu, D. F., Wu, L. F., Wang, J. H., Sun, Y. R., Zhang, M., & Zhang, Y. S. (2011). Thermal behavior and viscoelastic properties of poly(phenylene sulfide)/epoxy resin mixture. *Materials Chemistry and Physics*, *128*, 274–282.
Wu, D. F., Wu, L., Wu, L. F., Xu, B., & Zhang, M. (2007). Non-isothermal cold crystallization behavior and kinetics of polylactide/clay nanocomposites. *Journal of Polymer Science Part B: Polymer Physics*, *45*, 1100–1113.
Wu, D. F., Wu, L., & Zhang, M. (2007). Rheology of multi-walled carbon nanotube/poly(butylene terephthalate) composites. *Journal of Polymer Science Part B: Polymer Physics*, *45*, 2239–2251.
Wu, D. F., Zhou, C. X., Yu, W., & Xie, F. (2005). Effect of flocculated structure on rheology of poly(butylene terephthalate)/clay nanocomposites. *Journal of Polymer Science Part B: Polymer Physics*, *43*, 2807–2818.
Wu, D. F., Zhou, C. X., Zheng, H., Mao, D. L., & Zhang, B. (2005). Study on rheological behavior of poly(butylene terephthalate)/montmorillonite nanocomposites. *European Polymer Journal*, *41*, 2199–2207.
Xu, C. J., Chen, J. X., Wu, D. F., Chen, Y., Lv, Q. L., & Wang, M. Q. (2016). Polylactide/acetylated nanocrystalline cellulose composites prepared by a continuous route: A phase interface-property study. *Carbohydrate Polymers*, *146*, 58–66.
Zhang, W., Dehghani-Sanij, A. A., & Blackburn, R. S. (2008). IR study on hydrogen bonding in epoxy resin-silica nanocomposites. *Progress in Natural Science*, *18*, 801–805.